SUPPORTING INFORMATION

A conserved arginine with non-conserved function is a key determinant of agonist selectivity in α7 nicotinic acetylcholine receptors

Teresa Minguez-Viñas[a], Beatriz E. Nielsen[b], Deborah K. Shoemark[c], Cecilia Gotti[d], Richard B. Sessions[c], Adrian J. Mulholland[e], Cecilia Bouzat[b], Susan Wonnacott[f], Timothy Gallagher[e], Isabel Bermudez[a]*, A Sofia Oliveira[c][e]**

[a]Department of Biological and Medical Sciences, Oxford Brookes University, Oxford OX3 0BP (United Kingdom); [b]Instituto de Investigaciones Bioquímicas de Bahía Blanca, Departamento de Biología, Bioquímica y Farmacia, Universidad Nacional del Sur-Consejo Nacional de Investigaciones Científicas y Técnicas (CONICET), Bahía Blanca 8000 (Argentina); [c]School of Biochemistry, University of Bristol, Bristol BS8 1DT (United Kingdom); [d]CNR, Institute of Neuroscience, Biometra Department, University of Milan, I-20129 Milan (Italy); [e]School of Chemistry, University of Bristol, Bristol BS8 1TS (United Kingdom); [f]Department of Biology and Biochemistry, University of Bath, Bath BA2 7AY (United Kingdom).

Corresponding authors:

* ibermudez@brookes ** sofia.oliveira@bristol.ac

TABLE OF CONTENTS

1. Supporting Figures

Figures S1 to S15

2. Supporting Tables

Tables S1 to S3

1. Supporting Figures

Figure S1. **A)** The nAChR structure and the agonist binding pocket. The structure shown here corresponds to the crystal structure of the α4β2 nAChR (PDB code: 5KXI) (Perez-Morales et al., 2016). The principal subunit (α4) is shown in blue, and the complementary subunit (β2) is shown in orange. The structure includes the transmembrane domain and the ECD with the inset showing a close-up view of the agonist binding pocket with loops A-C in the principal subunit and loops D-F in the complementary subunit highlighted. Note that although historically known as loops, loops E and D are indeed β3-strands. **B)** Binding mode of ACh, cytisine and 10-methylcytisine in α4β2 and α7 nAChRs. Agonists are represented as balls-and-sticks, and the tryptophan residue (TrpB) that provides the anchor point for the agonist in the binding site is shown with sticks.

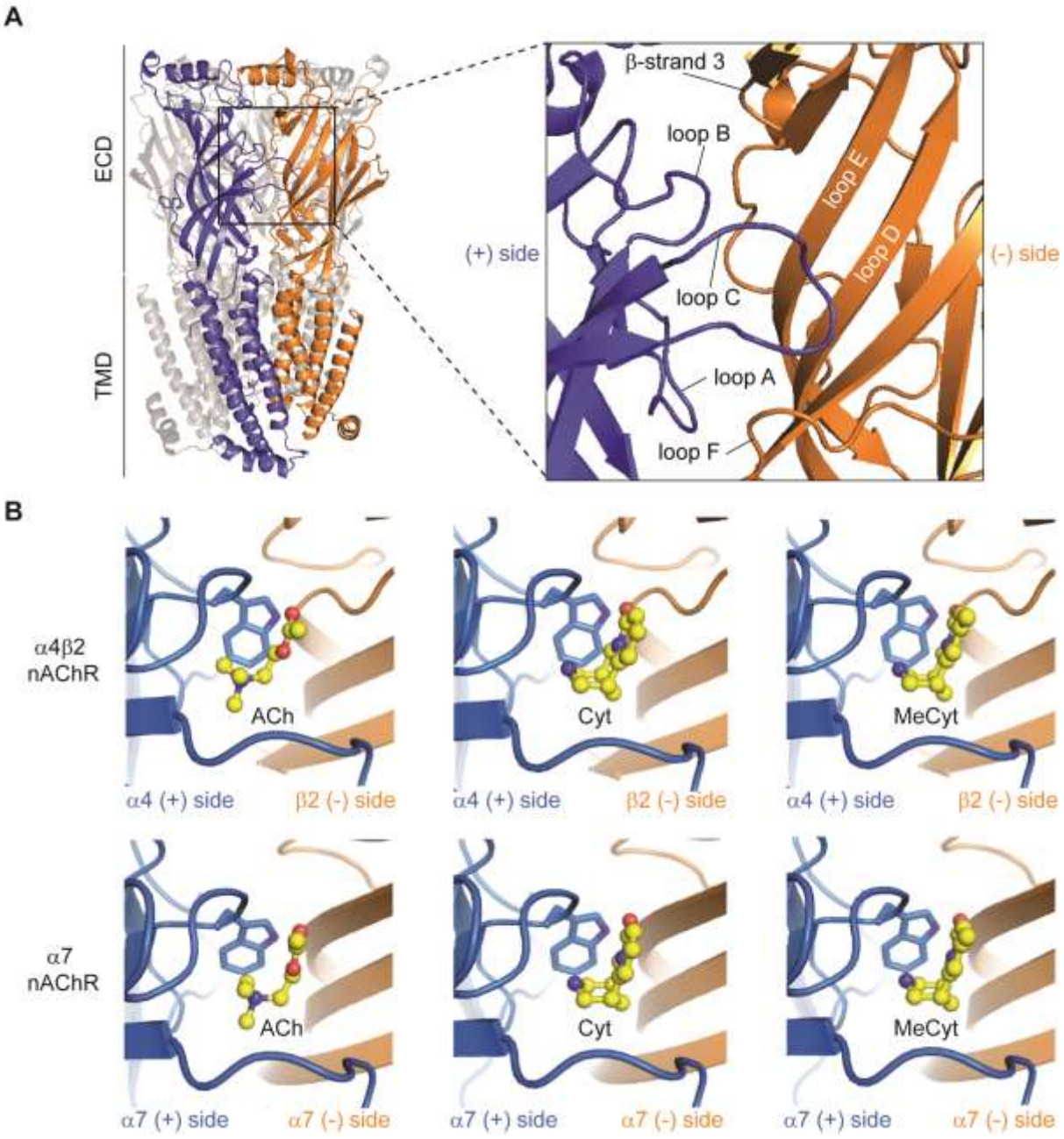

Figure S2. Representative dwell time histograms of single-channel recordings from α7, α7G174D and α7R101A activated by Ach (top) or cytisine (bottom). Dwell times are shown on logarithmic time axes with overlaid fits to the sum of exponentials (solid line, fits; dotted lines, individual components). Burst duration histograms are open time histograms generated by summing open times with flanking closings briefer than a critical time determined from corresponding closed time histograms (see Methods). Membrane potential: -70 mV. Abbreviations: cytisine, Cyt; 10-methylcytisine, MeCyt.

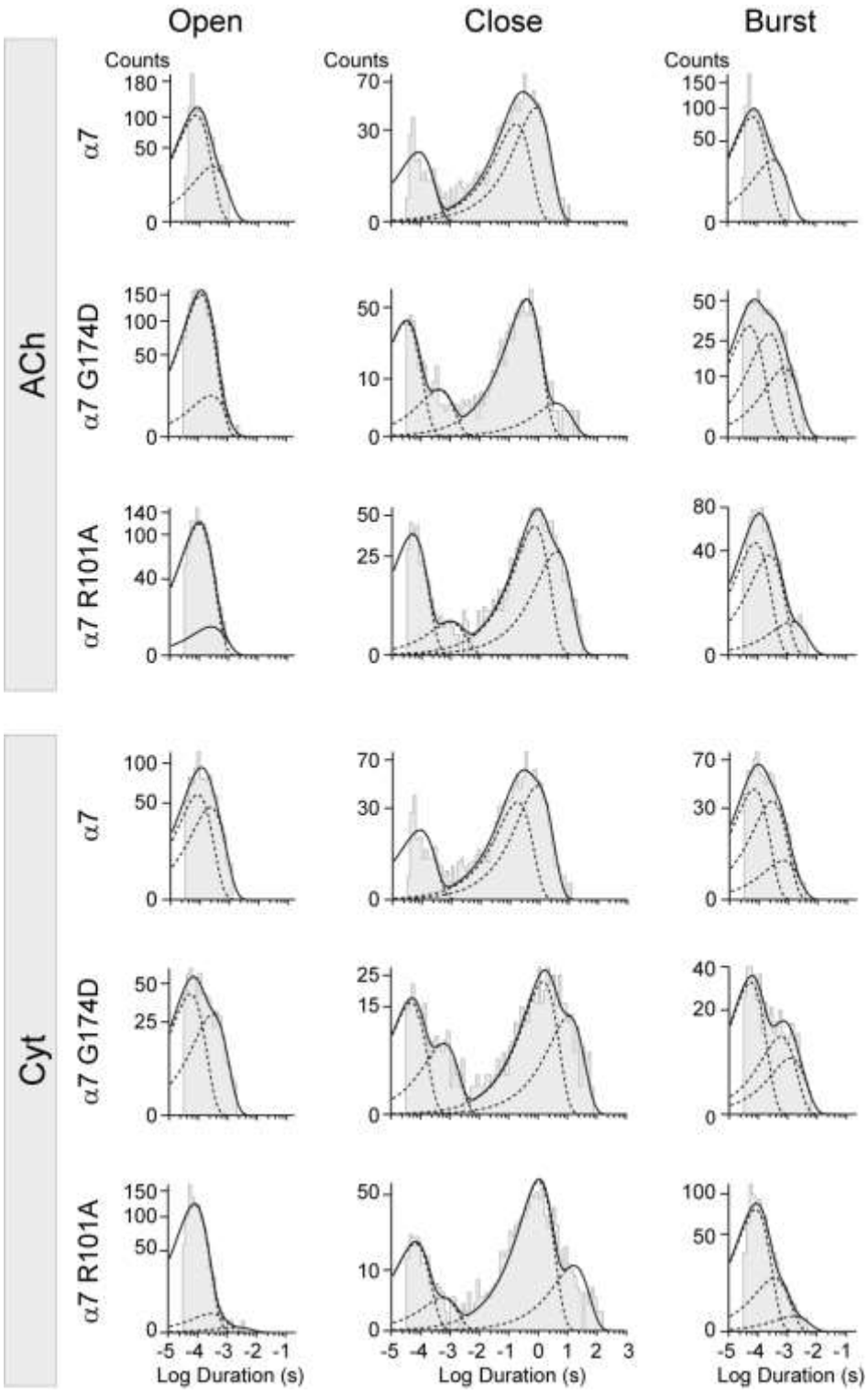

Figure S3. Temporal evolution of the average C_α RMSD for the α4β2 systems. The C_αRMSD was calculated relative to the starting structures, and the averages were obtained over all replicates. Agonist shown are **A)** ACh, **B)** cytisine and **C)** 10-methylcytisine. Abbreviations: cytisine, Cyt; 10-methylcytisine, MeCyt.

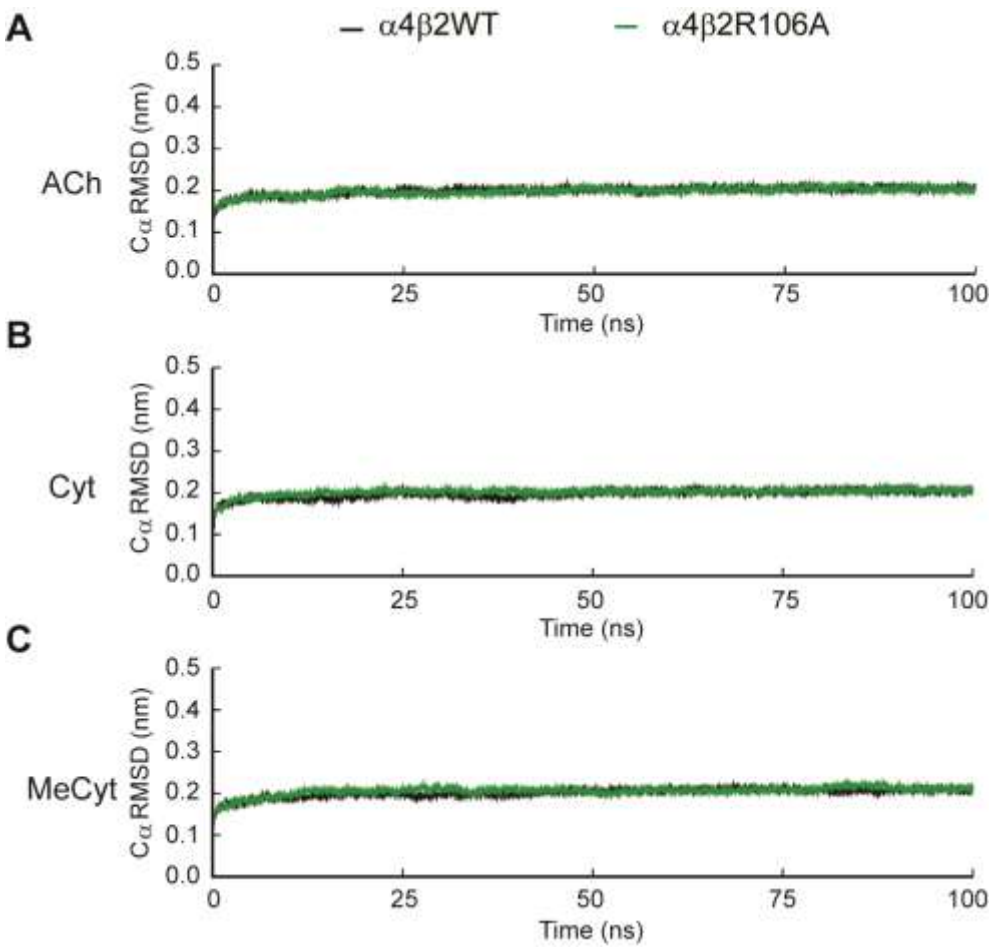

Figure S4. Temporal evolution of the average C_α RMSD for the α7 systems. The C_αRMSD was calculated relative to the starting structures, and the averages were obtained over all replicates. Agonist shown are **A)** ACh, **B)** cytisine and **C)** 10-methylcytisine. Abbreviations: cytisine, Cyt; 10-methylcytisine, MeCyt.

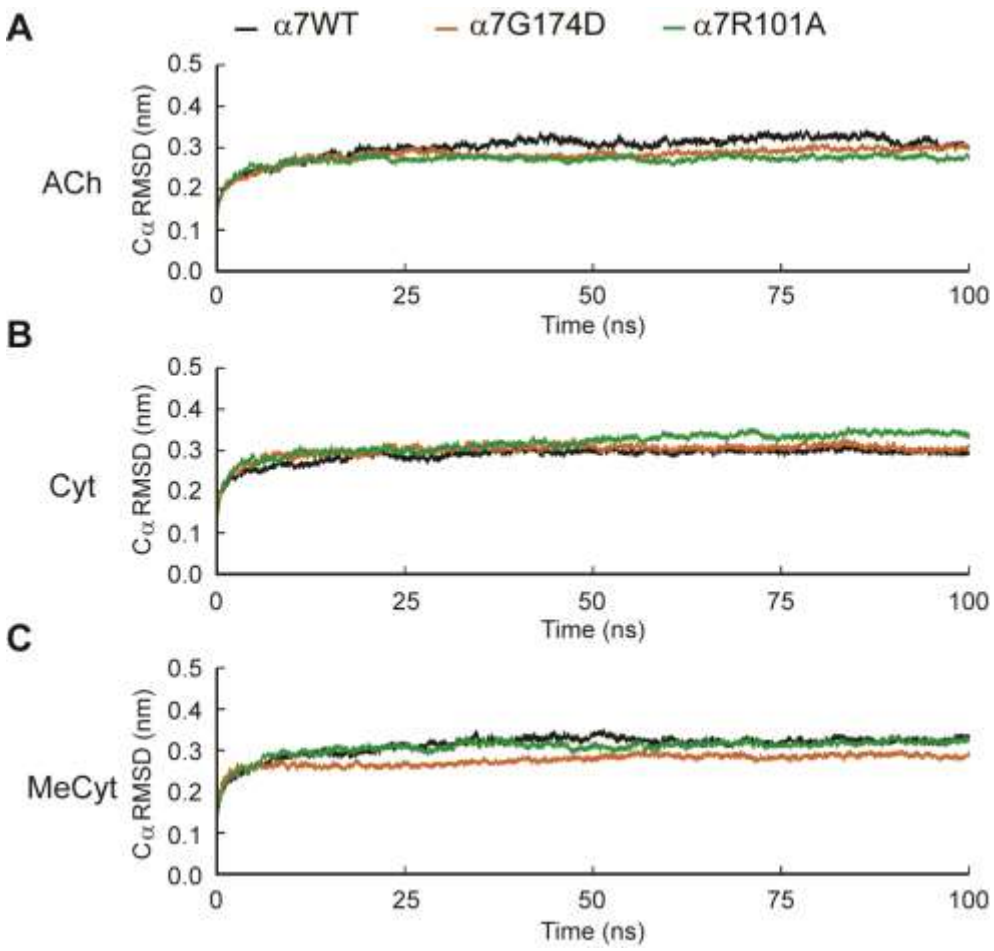

Figure S5. Probability density maps for the side chain of arginine R106 in the β2 subunit and R101 in the α7 nAChR complexes of the **A)** first and **B)** second of the two non-consecutive agonist binding pockets analysed. The complexes are bound to ACh, cytisine or 10-methylcytisine. No noticeable differences are observed between the maps for the two binding sites. The contours at 0.00001 $Å^{-3}$ for the Cζ are depicted as a blue mesh. Abbreviations: cytisine, Cyt; 10-methylcytisine, MeCyt.

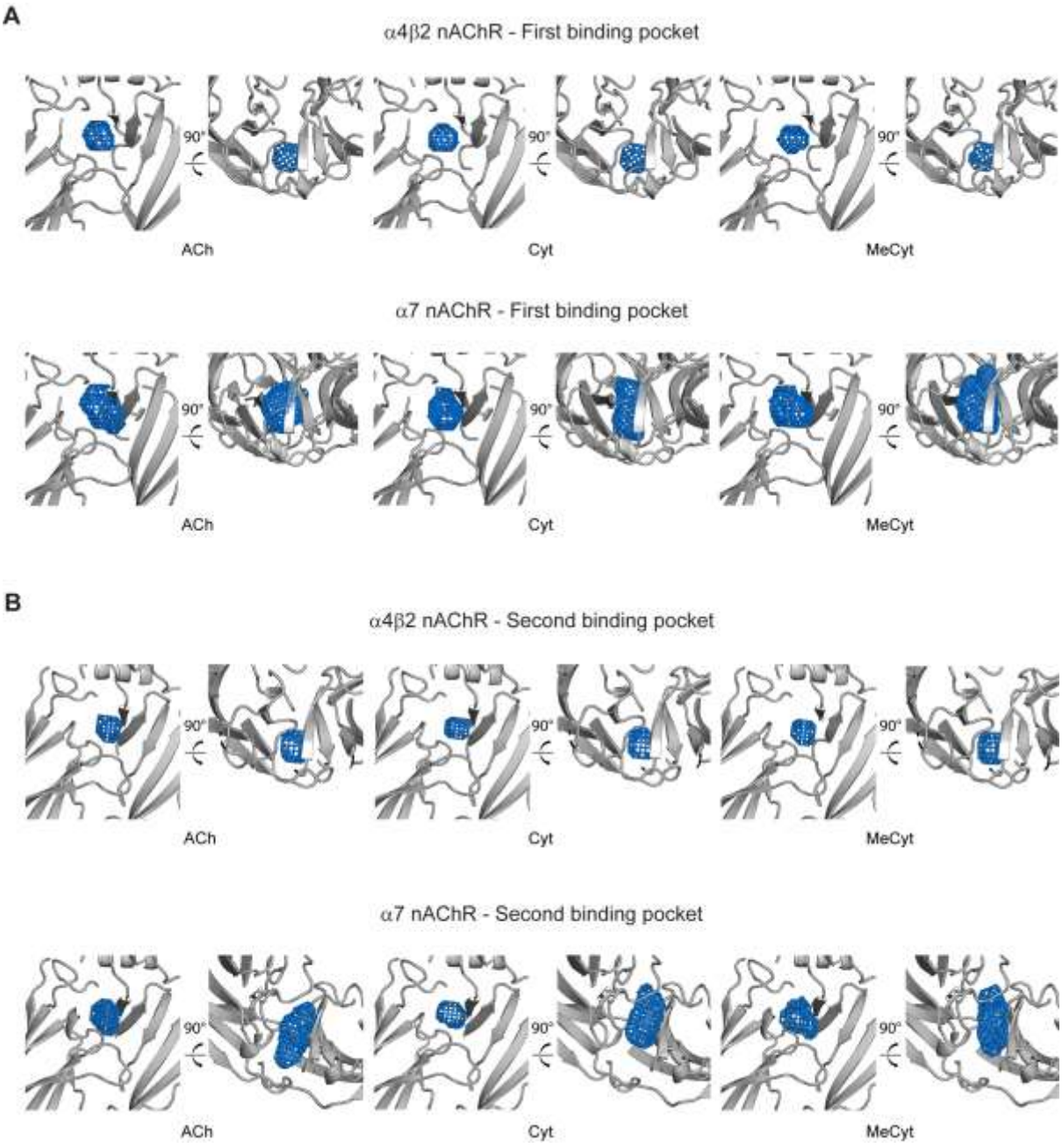

Figure S6. Distribution of the minimum distance between the conserved arginine in β3-strand (R101 in α7 and R106 in α4β2) and **A)** 10-methylcytisine, **B)** TyrA, **C)** TrpB, **D)** TyrC1, **E)** TyrC2 and **F)** TrpD in the α7 (black line) and α4β2 (orange line) systems. The histograms reflect the distances over the two binding pockets. Note that these distance profiles clearly show a distinct pattern of behavior for the β3-strand arginine between the α7 and α4β2 receptors. Abbreviations: 10-methylcytisine, MeCyt.

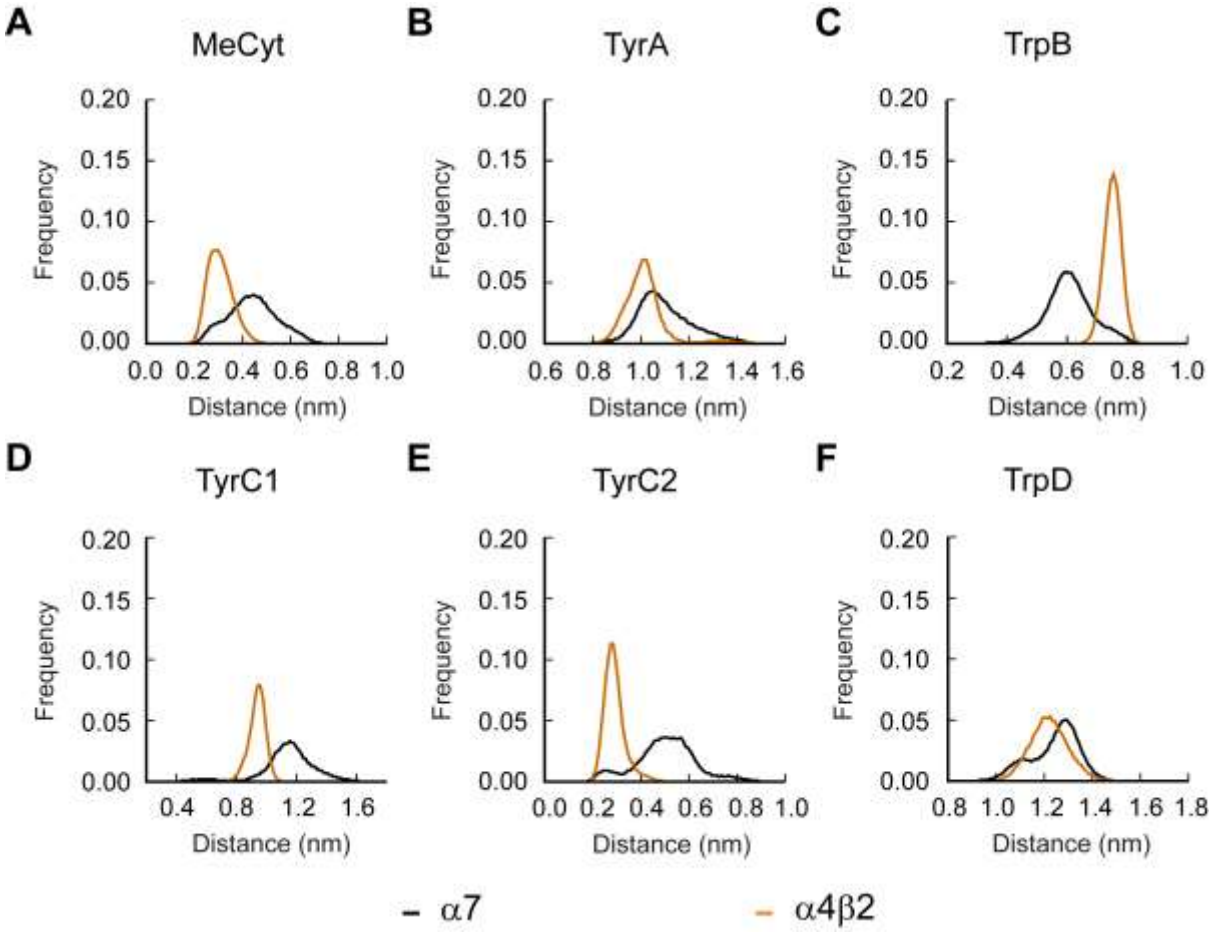

Figure S7. Sequence alignment for loop B and β3-strand residues of nAChR subunits. The arginine residue in β3-strand is highly conserved in the nAChR family, whereas the aspartate in loop B is conserved by subunits that contribute the principal side of the agonist sites in heteromeric receptors, except for the α9 and α10 subunits.

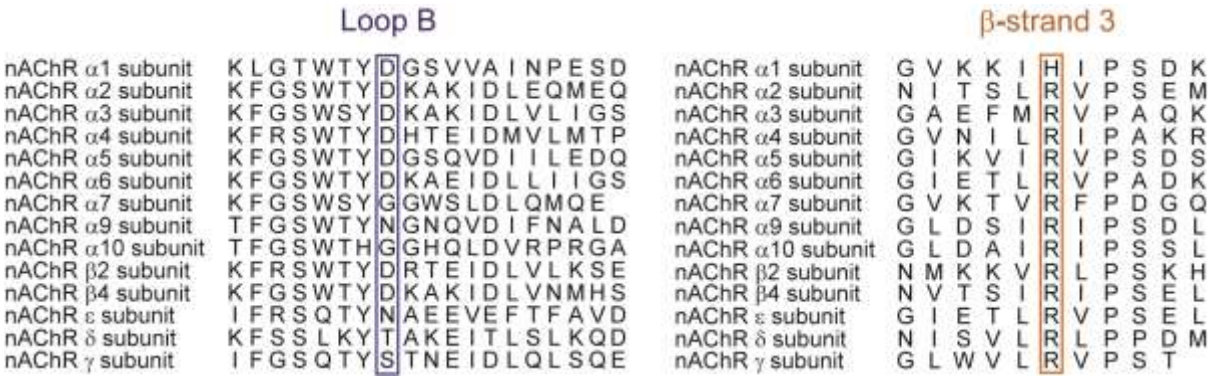

Figure S8. Statistical correlations for the residue in position 174 for the α7 and mutant α7G174D receptor complexes with ACh, cytisine or 10-methylcytisine bound. Correlated motions for the residue in position 174 in the **A)** first and **B)** second binding pocket. The correlations between the Cα atom of residue 174 in the principal subunit and all the remaining Cα atoms are shown. Note that the atoms that systematically move along the opposite direction as residue 174 have a correlation value of -1 whereas those systematically moving along the same direction show a correlation of 1. The atoms whose movements relative to residue 174 are uncorrelated present a correlation value of 0. The location of residue 174 is highlighted with a sphere. Abbreviations: cytisine, Cyt; 10-methylcytisine, MeCyt.

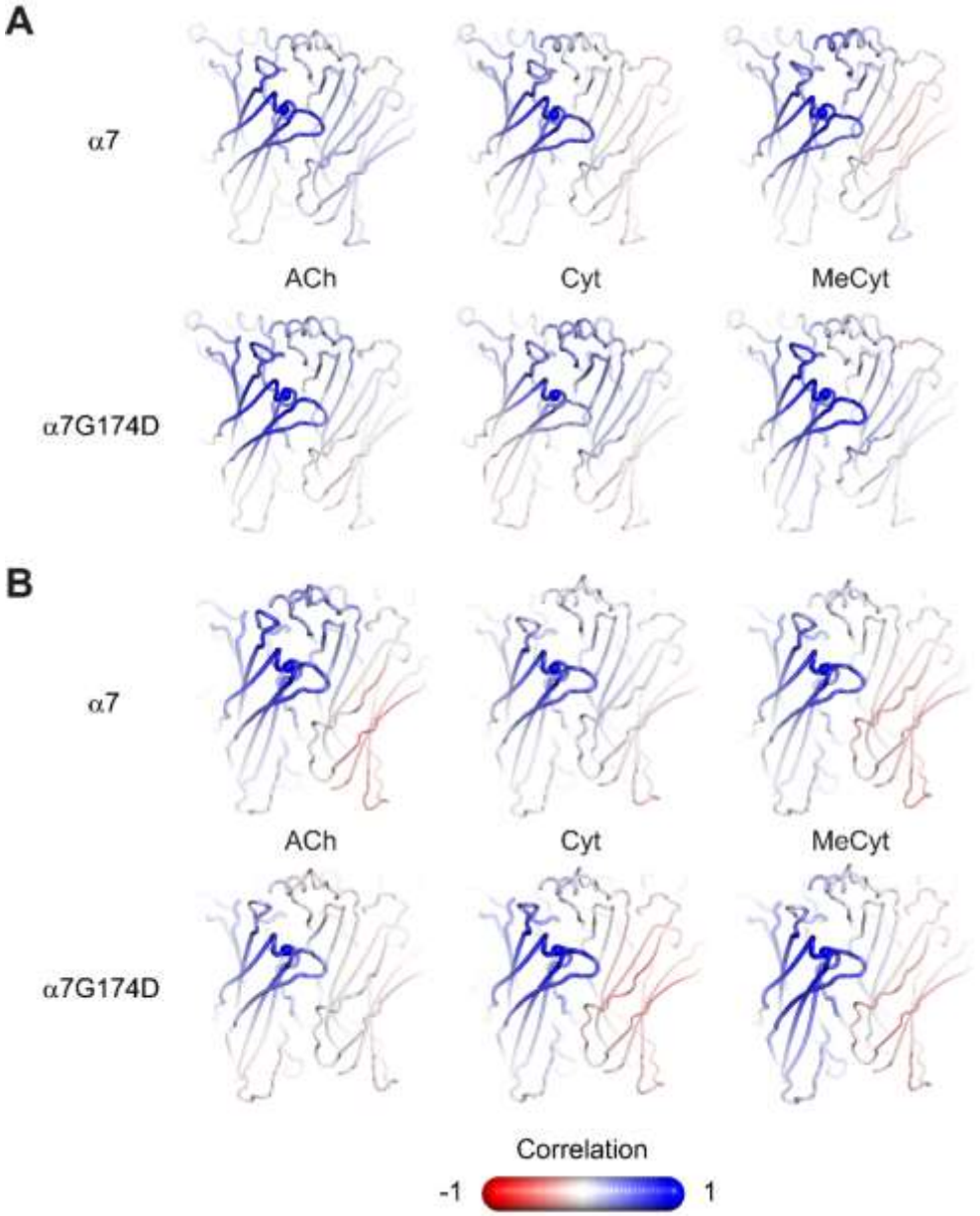

Figure S9. Average change in Cα RMSF between the α7 and α7G174D systems with ACh, cytisine or 10-methylcytisine bound in the **A)** first and **B)** second binding pocket. The RMSF differences for the principal (left side image) and complementary (right side image) subunits are shown for the two agonist binding sites. Note that the complexes with cytisine and, particularly 10-methylcytisine, the largest dynamical differences in the binding pockets were located around the R101 region and in loop E. Please zoom into the image for detailed visualization. Abbreviations: cytisine, Cyt; 10-methylcytisine, MeCyt.

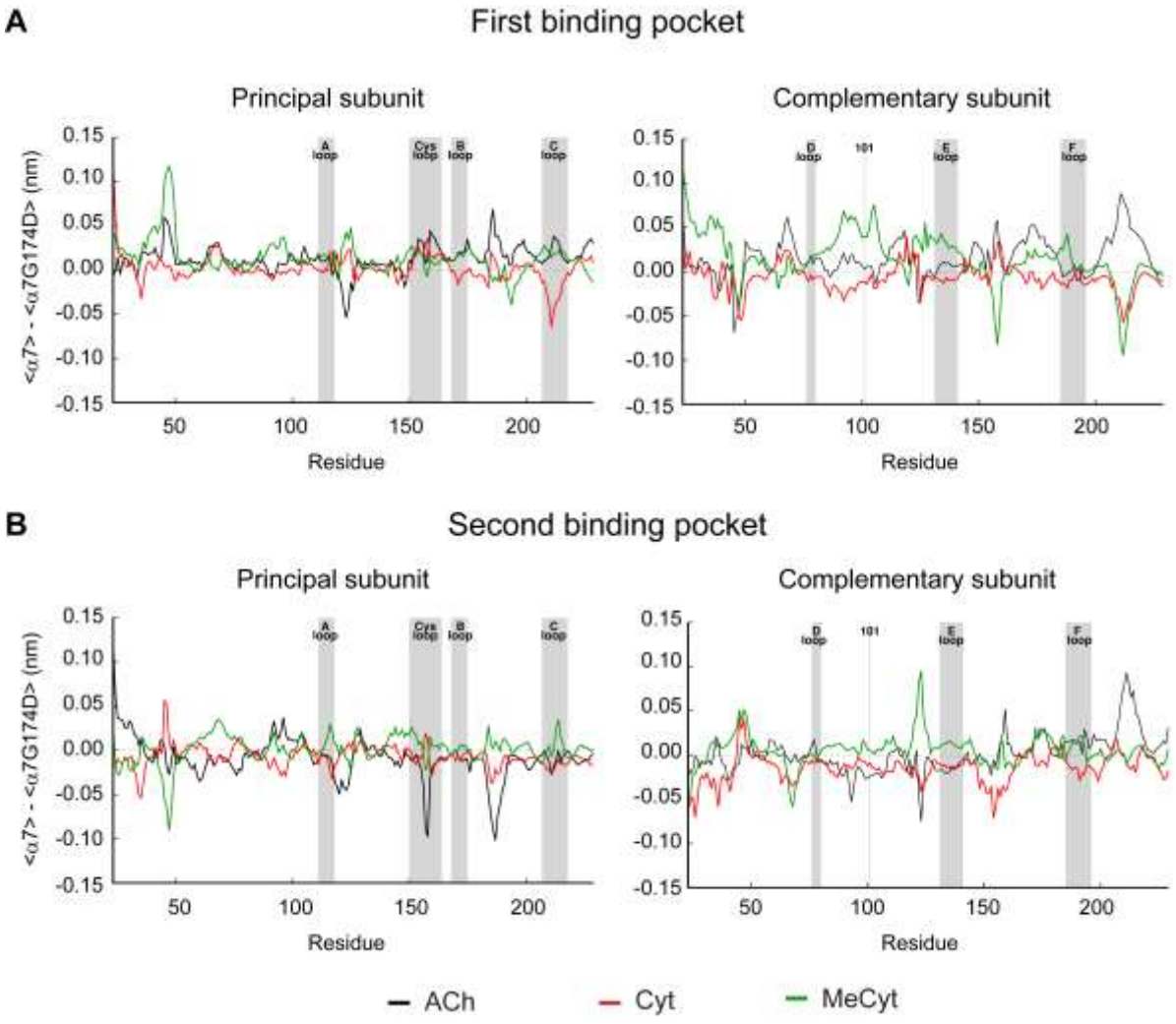

Figure S10. Distribution of the distance between **A)** ACh, **B)** cytisine and **C)** 10-methylcytisine and the main conserved aromatic residues lining the binding pockets in the α7 (black line) and α7G174D (orange line) systems. Overall distribution of the distance between the sidechain of TyrA (α7115), TrpB (α7W171), TyrC1 (α7Y210), TyrC2 (α7Y217) or TrpD (α7W77) and the charged N atom of the agonists. The histograms reflect the distances over the two binding pockets. Note that for ACh-bound systems, the differences in the Y115 and W77 distance profiles between the α7 and α7G174D receptors are subtle, probably because the high mobility and small size of ACh makes the binding interactions of this agonist more tolerant of structural changes. In contrast, for cytisine and 10-methylcytisine, differences in the distance profiles are observed. In particular, for cytisine, the changes in the Y115 and W77 profiles between the α7 and α7G174D receptors are substantial. Abbreviations: cytisine, Cyt; 10-methylcytisine, MeCyt.

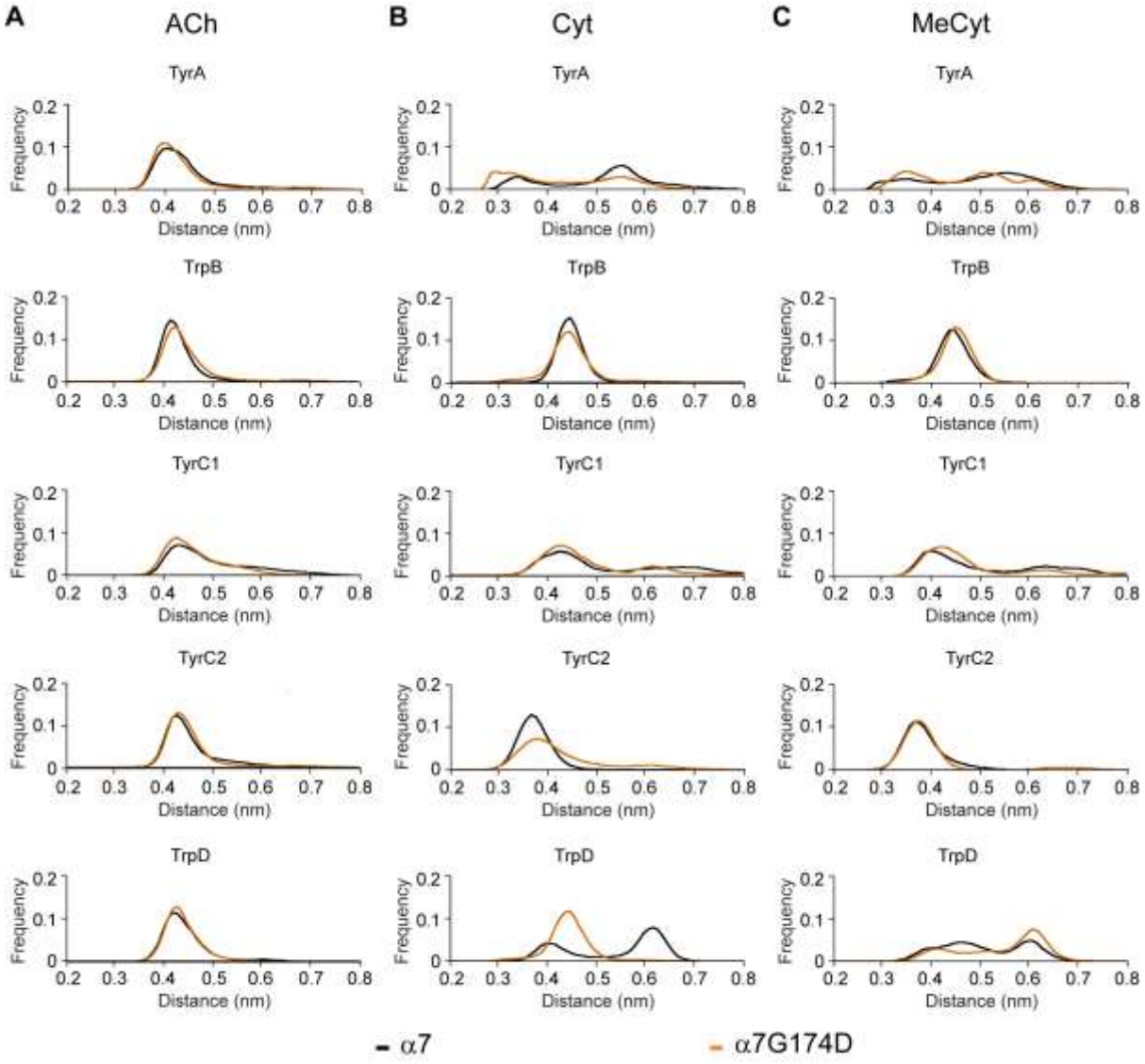

Figure S11. **A)** Average change in Cα RMSF between the α7 and α7R101A systems with ACh (black line) cytisine (red line) or 10-methylcytisine (green line) bound to the second non-consecutive binding pocket of the receptors. The RMSF differences for the principal (left side image) and complementary (right side image) subunits are shown. Please zoom into the image for detailed visualization. **B**) Average RMSF difference between α7 and α7R101A systems bound to ACh, cytisine or 10-methylcytisine mapped into the average structure of each system. The structure colours are related to the average Cα RMSF: the red and blue regions correspond to the residues with the largest differences between the two systems. Abbreviations: cytisine, Cyt; 10-methylcytisine, MeCyt.

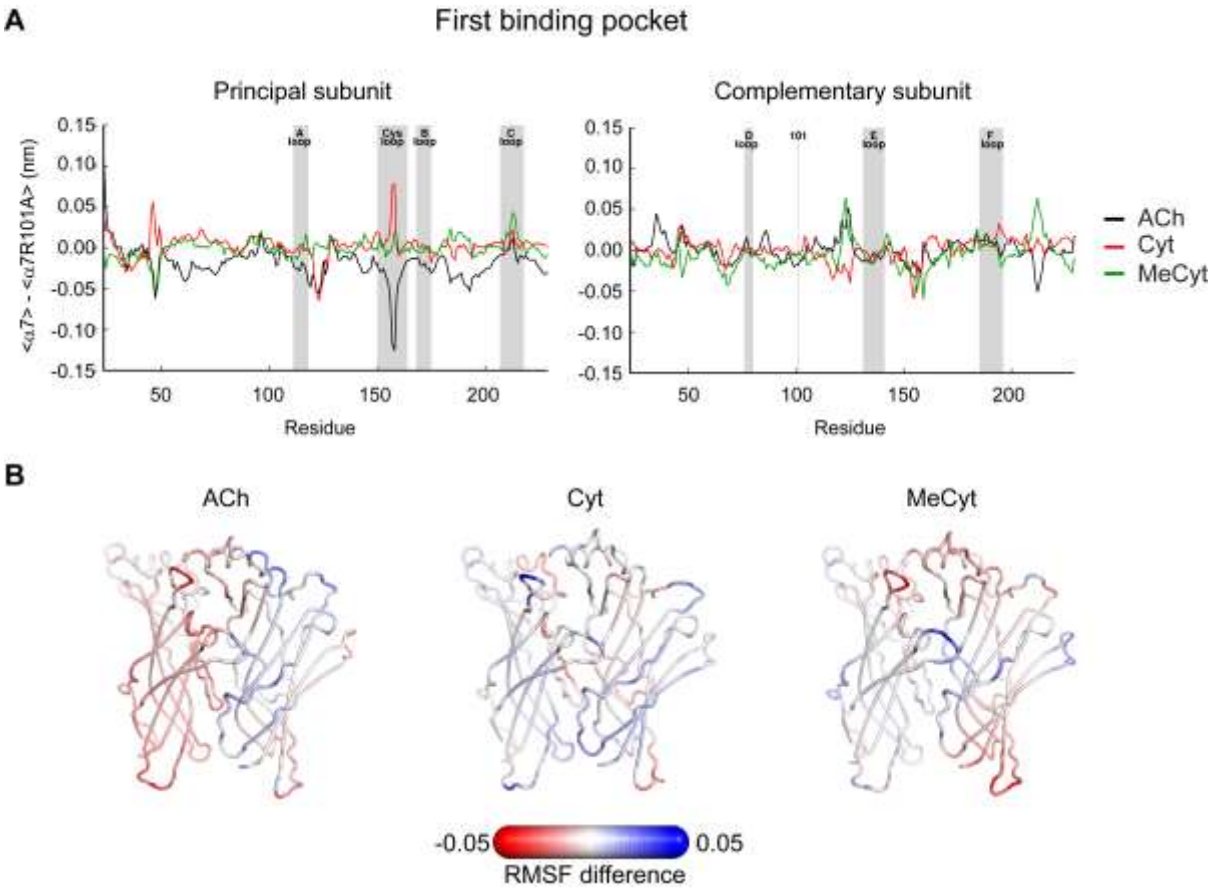

Figure S12. Average structure of agonist-bound α7 and α7R101A complexes**.** The agonist simulated were **A)** ACh, **B)** cytisine and **C)** 10-methylcytisine bound to the second non-consecutive binding pocket of the receptor. In this image, α7R101A structures are colored in blue, whereas the α7 ones are shown in grey. Note that for the cytisine-bound α7R101A complex, there is a clear change in the extent of loop C capping, compared to α7 wild type nAChR. The structures shown here represent the average structure calculated over all replicates for each system, as described in the the Methods section of main manuscript. Abbreviations: cytisine, Cyt and 10-methylcytisine, MeCyt.

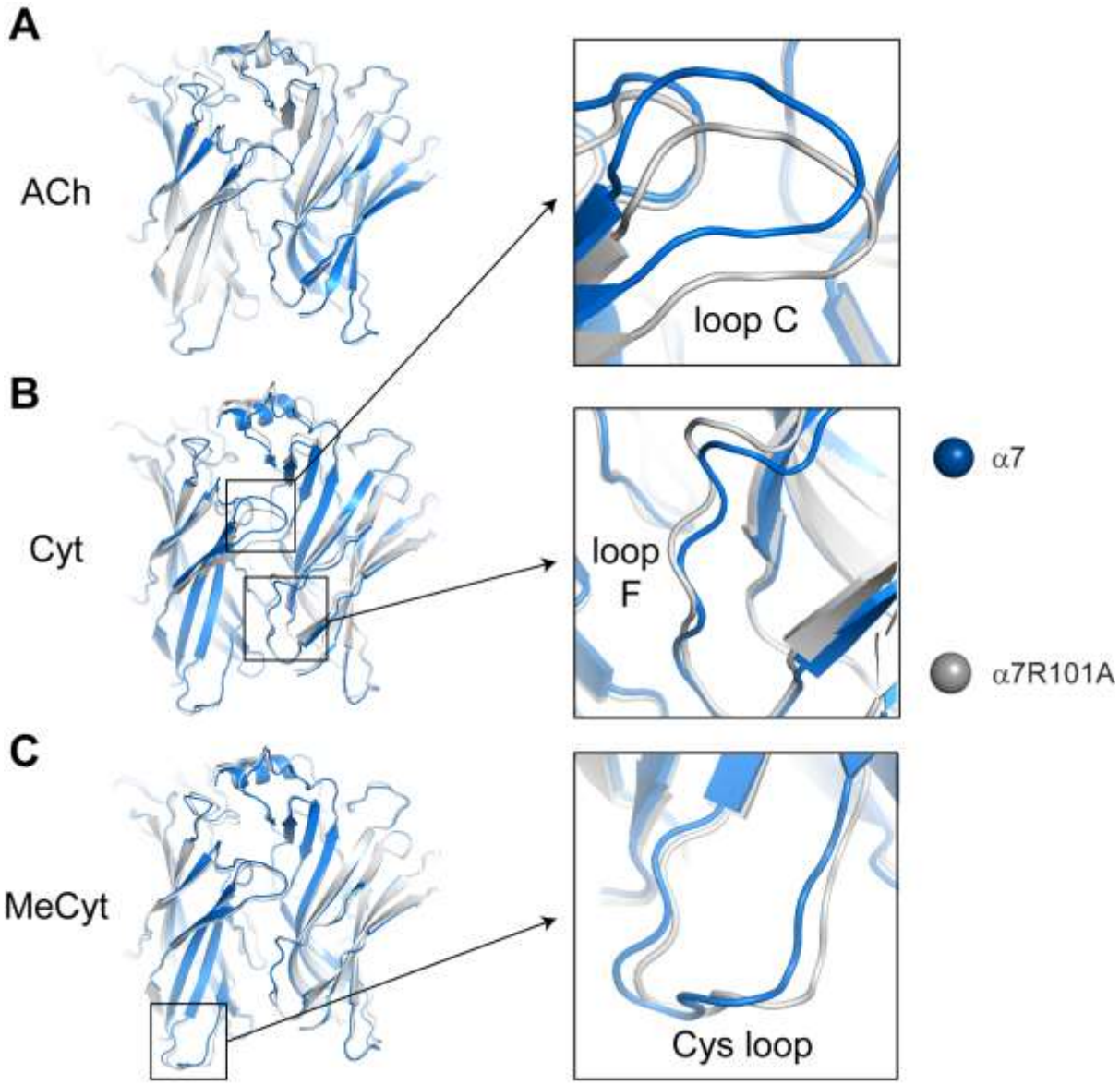

Figure S13. Comparison of loop C E215 and β3-strand K98 interaction in the α7 and α7R101A receptors. **A)** Homology model of the α7 nAChR (left panel) with the inset showing a close-up view of the agonist pocket. Note position of the side chains of R101, E215 and K98. The principal and complementary subunits are coloured in blue and orange, respectively. The residues numbering refers to the UniProt sequence codes: P36544 (α7 subunit cDNA). **B)** Overall distribution of the minimum distance between the sidechains of E215 and K98 in the wild type α7 receptor in the presence of ACh (black line), cytisine (red line) or 10-methylcytisine (green line). **C)** Overall distribution of the minimum distance between the sidechains of E215 and K98 in the α7R101A receptor in the presence of ACh (black line), cytisine (red line) or 10-methylcytisine (green line). The histograms shown in B) and C) reflect the distances over the two binding pockets. Abbreviations: cytisine, Cyt; 10-methylcytisine, MeCyt.

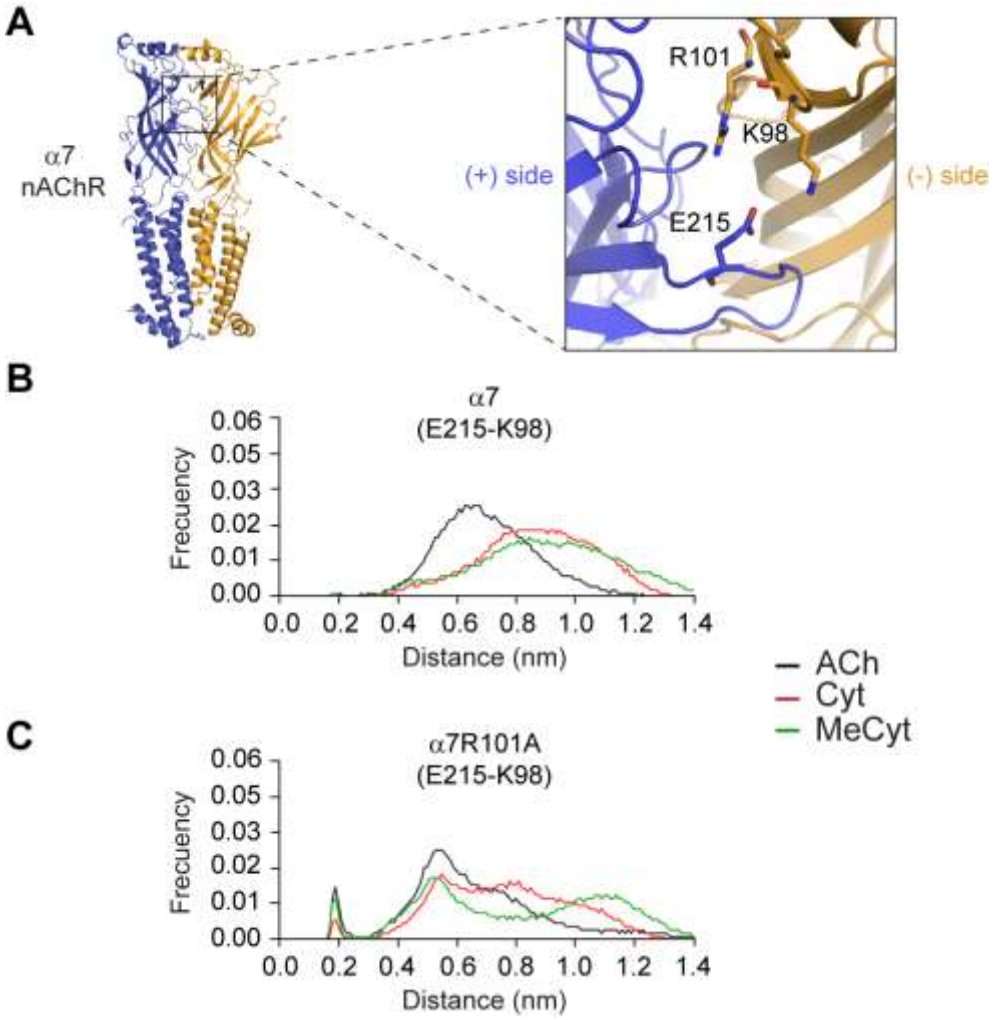

Figure S14. Distribution of the distance between the agonists and the main aromatic residues forming the binding pockets in the α7 and α7R101A receptors. **A)** Overall distribution of the distance between the sidechain of TrpB (W171 in the α7 subunit) and the charged N atom of the ligands. **B)** Overall distribution of the distance between the sidechain of TyrA (Y115 in the α7 subunit) and the charged N atom of the ligands. The histograms reflect the distances over the two binding pockets. Abbreviations: cytisine, Cyt; 10-methylcytisine, MeCyt.

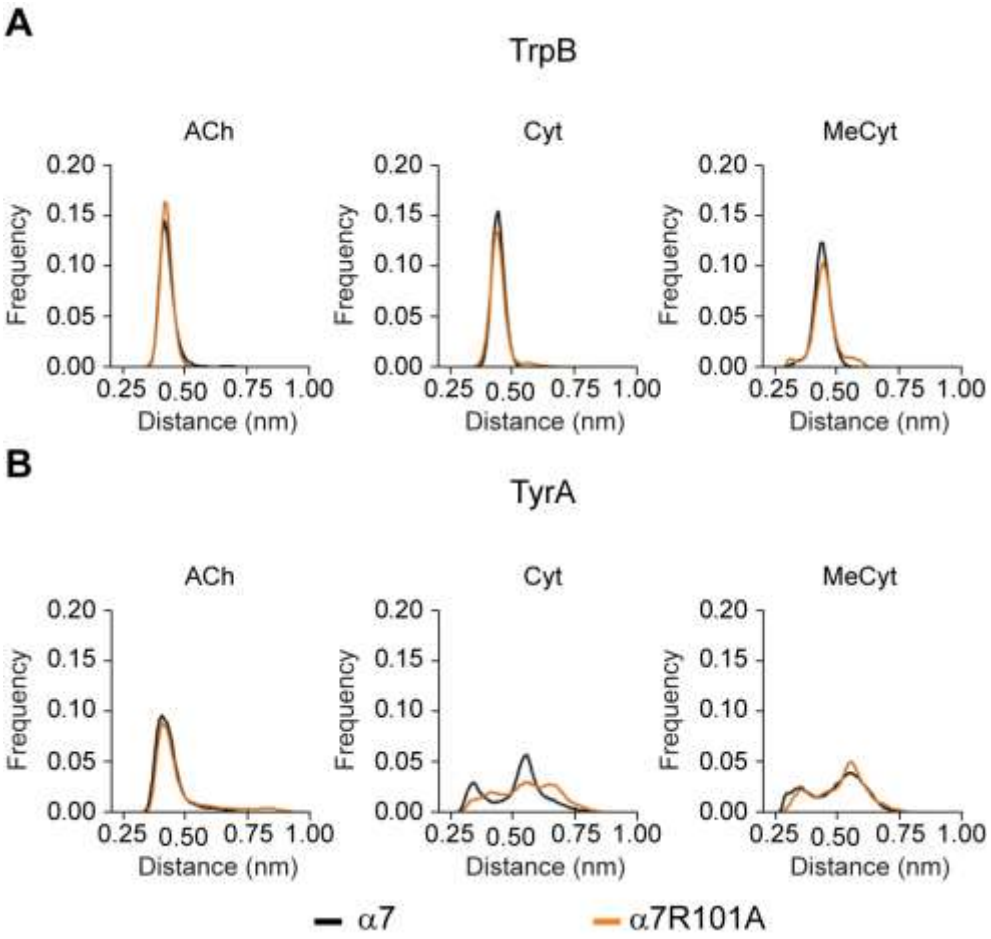

Figure S15. Electrostatic maps for α7 and α4β2 receptors and their respective arginine mutants. **A)** α7 (left panel) and α7R101A (right panel) nAChRs and **B)** α4β2 (left panel) and α4β2R106A (right panel) receptors. Zoom of the electrostatic potential distribution on the top of the agonist site. The potential varies between -15 and +15 KT/e, as shown in the colour-reference bar, with red and blue representing negative and positive potentials, respectively. In both α7 and α4β2 subtypes, the substitution of the long positively charged side chain of arginine in β3-strand by a short neutral side chain of alanine leads not only to a change in the shape and size of the binding site but also in the charge distribution surrounding the orthosteric binding pocket. Note, however that β3-strand arginine shows distinct dynamic behaviours between the α7 and α4β2 nAChRs (Figure S5). In the α4β2 nAChR, the side-chain of R106 shows reduced dynamics as it involved in a strong inter-subunit salt-bridge with D185. In the α7 nAChR, the side-chain of R101 exhibits high mobility being even able to orient towards the inside of the binding pocket, which may further impact the electrostatic landscape of that region.

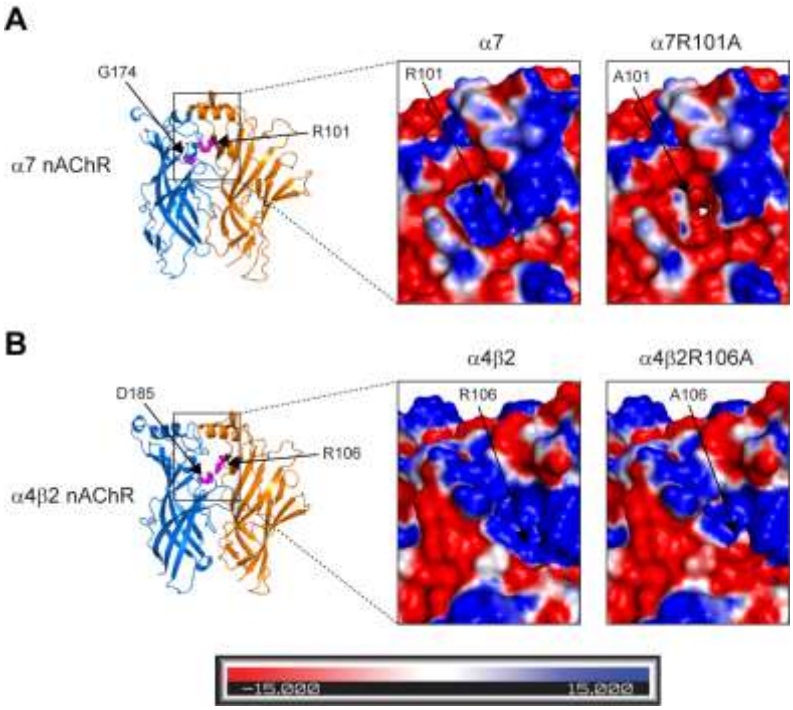

2. Supporting Tables

Table S1. Sensitivity of wild type and mutant α7 nAChRs to activation by agonists. Recently, we have shown that even though cytisine and its C(10)-methyl variant share the same core-binding interactions with conserved residues in the α7 and α4β2 nAChRs (Rego-Campello et al., 2018), 10-methylcytisine display negligible binding to α7 receptors. By superimposing structural models of the agonist pocket of α4β2 and α7 receptors bound to 10-methylcytisine**,** we observed differences in a layer of non-agonist binding residues in the binding pocket, namely β2F144 *vs* α7Q139, β2V136 *vs* α7L131, β2A65 *vs* α7L60, α4T183 *vs* α7S172 and β2S133 *vs* α7T128 (A) (Rego-Campello et al., 2018) Note that the sequence numbering that we use for α7 (UniProt code P36544), α4 (UniProt code P43681) and β2 (UniProt code P17787) cDNAs includes the signal sequence. Given that these residues could modify hydrogen bonding patterns, hydrophobicity or volume of the agonist pocket, which could affect agonist binding, we tested if making α7 receptors α4β2-like in respect of these residues could increase the potency of 10-methylcytisine for α7 receptors. However, functional assays of α7 nAChR bearing these α4β2 residues do not display higher sensitivity to activation 10-methylcytisine. Whole-cell current responses to agonist were measured using *Xenopus laevis* oocyte two electrode voltage clamping electrophysiology. The agonists tested were ACh, cytisine and 10-methylcytisine. The nucleus of oocytes was injected with wild type or mutant α7 subunit cDNA. Data were fitted with the empirical Hill equation, as described in Methods section of the main manuscript. The estimated parameters EC_{50} and I_{max}/I_{AChMax} represent the means (95% CI) of 8-10 independent experiments carried out using 5 different oocyte donors. Statistical analysis was performed by comparing the estimated values of WT and mutant EC_{50} and I_{max}/I_{AChMax} using ANOVA followed by Dunnett's post-test. Asterisks indicate level of statistical difference from wild type (*$p < 0.05$). ND, not determined.

Receptor	**ACh**		**Cytisine**		**10-Methylcytisine**	
	EC_{50} (μM) (95% CI)	**I_{max}/I_{AChMax} (95% CI)**	**EC_{50} (μM) (95% CI)**	**I_{max}/I_{AChMax} (95% CI)**	**EC_{50} (μM) (95% CI)**	**I_{max}/I_{AChMax} (95% CI)**
α7	82.4 (71-95)	1	29.64 (24-37)	0.93 (0.9-0.94)	643 (493-837)	0.55 (0.4-0.7)
α7L60A, L131V	50.0 (19-134)	1	66.2 (23-191)	0.9 (0.7-1.2)	ND	0.70
α7Q139F	462* (340-628)	1	137* (21-254)	1.11 (1.0-1.2)	504 (301-545)	0.35 (0.1-0.6)
α7T128S, S172T	367.3* (232-581)	1	91.2* (57-271)	1.10 (0.8-1.4)	972.7* (321-2944)	0.74 (0.5-1.0)

Table S2. An inter-subunit salt-bridge between α4D185 and β2R106 is necessary for receptor expression. Dismantling the α4D185-β2R101 salt-bridge by the introduction of D185G or R106A ablated functional expression of the $(\alpha4)_2(\beta2)_3$ and decreased functional expression of $(\alpha4)_3(\beta2)_2$ by about 14-fold. To estimate functional expression, we compared the amplitude of the currents elicited by 1mM ACh (a maximal ACh concentration at $(\alpha4)_3(\beta2)_2$ and $(\alpha4)_2(\beta2)_3$ receptors as well as at mutant $(\alpha4^{D185G})_2(\beta2)_3$ and $(\alpha4)_2(\beta2^{R106A})_3$ receptors). The overall amount of cDNA mixture injected was kept the same for all receptors assayed (5 ng). To favour the expression of the 3α4-2β2 stoichiometry, the cDNAs were injected at 10α4: 1β2 ratio, whereas for the 2α4-3β2 stoichiometry, the ratio was 1 α4 ; 10 β2. Maximal currents were elicited with 1 mM ACh, a maximal ACh concentration at wild type and the mutant α4β2 receptors. The current responses of mutant and wild type receptors were measured on the same day using the automated two-electrode voltage clamp HiClamp system, as described in the Methods section of the manuscript. The I/IAChmax data shown are the means ± SEM obtained from 18 recordings carried out using 6 different oocyte donors (n = 18; N = 6). The concentration-response data for ACh were fitted with the Hill equation as detailed in the Method section of the main manuscript; the EC_{50} shown were obtained from n = 10 independent recordings and using N = 5 oocyte donors. The reduced level of functional expression impeded the construction of reliable activation concentration-response relationships for cytisine and 10-methylcytisine. These ligands behave as poorly efficacious partial agonist at the two forms of the α4β2 receptors. Therefore, to assess the impact of dismantling the D-R salt bridge on the functional potency of cytisine and 10-methylcytisine, we evaluated the ability of these ligands to act as competitive antagonists. This strategy is based on the rationale that partial agonists, such as cytisine and 10-methylcytisine, fully occupy the agonist binding site while having low efficacy in activating the receptor. When in the binding site, a ligand will prevent other agonists from binding and activating the receptor, thus in this circumstance the partial agonist also acts as a partial competitive antagonist. Neither D185G nor R106A affected the inhibitory potency of cytisine or 10-methylcytisine, compared to wild type (n = 8; N= 5). [^{3}H]Epibatidine binding assays on cells expressing α4β2 receptors showed a five-fold decrease in Bmax but no changes in Kd. Data shown represent the mean of three independent experiments carried out in triplicate and using three different batches of cultured cell (n = 3; N = 3). Collectively, the data indicates that abolishing the D185-R106 salt bridge disturbs cell surface expression but not the binding affinity or efficacy of cytisine or 10-methylcytisine.

Whole-cell recordings				
Receptor	**I_{AChMax} ±SEM μA**	**ACh EC_{50} (μM) (95% CI)**	**Cytisine IC_{50} (μM) (95% CI)**	**10-methylcytisine IC_{50} (μM) (95% CI)**
$(\alpha4)_3(\beta2)_2$	1.8±0.6	60 (48-69)	13 (9-19)	13 (6-28)
$(\alpha4^{D185G})_3(\beta2)_2$	0.11±0.06	67 (54-84)	21 (11-40)	14 (7-29)
$(\alpha4)_3(\beta2^{R106A})_2$	0.09±0.01	53 (26-47)	25 (10-61)	14 (11-18)
$(\alpha4)_2(\beta2)_3$	0.8±0.1	7 (5.2-8.2)	0.56 (0.3-1.0)	0.73 (0.3-2.1)
$(\alpha4^{D185G})_2(\beta2)_3$	0.05±0.02	ND	ND	ND
$(\alpha4)_2(\beta2^{R106A})_3$	0.05±0.009	ND	ND	ND

[^{3}H]Epibatidine Binding		
Receptor	**K_d ± SEM (nM)**	**B_{max} ± SEM (fmol/mg of prot.)**
$\alpha4\beta2$	0.106 ±0.012	1219 ± 68
$\alpha4$D185G$\beta2$	0.149±0.013	269 ± 107

Table S3. Microscopic currents of wild type and mutant α7 nAChR.

Agonist	Receptor	τ_{open} (ms)	τ_{burst} (ms)	n	N
ACh	α7	0.27 ± 0.02	0.33 ± 0.06	6	5
	α7G174D	0.26 ± 0.10	0.69* ± 0.17	5	5
	α7R101A	0.29 ± 0.04	1.41* ± 0.41	5	5
Cytisine	α7	0.28 ± 0.09	0.72 ± 0.12	6	5
	α7G174D	0.31 ± 0.08	1.25* ± 0.30	4	5
	α7R101A	0.29 ± 0.10	2.00* ± 0.26	7	5

τ_{open} and τ_{burst} correspond to the longest components of the corresponding open time and burst duration histograms. Values are mean ± SD. n: number of independent experiments, each from different cell patches. N: number of cell transfections. Statistical significance was determined by comparing the mean value in the mutant receptor respect to the mean value in the wild type α7 receptor for each agonist, by two-tailed Student's t-test; *, denotes statistical difference at $p<0.05$. N corresponds to number of transfected cell batches used, and n is the number of recordings carried out.